AD-A140 208 MHD (MAGNETOHYDRODYNAMIC)SSIMULATION OF A COMET MAGNETOSPHERE(U) NAVAL RESEARCH LAB WASHINTTON DC J A FEDDER ET AL. 12 APR 84 NRL-MR-5306 1/1

UNCLASSIFIED F/G 12/1 NL

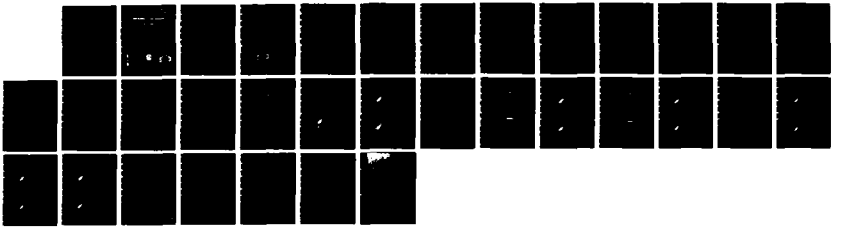

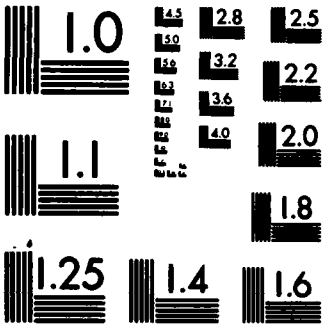

SECURITY CLASSIFICATION OF THIS PAGE

REPORT DOCUMENTATION PAGE

1a REPORT SECURITY CLASSIFICATION **UNCLASSIFIED**	1b RESTRICTIVE MARKINGS
2a SECURITY CLASSIFICATION AUTHORITY	3 DISTRIBUTION/AVAILABILITY OF REPORT **Approved for public release; distribution unlimited.**
2b DECLASSIFICATION/DOWNGRADING SCHEDULE	
4 PERFORMING ORGANIZATION REPORT NUMBER(S) **NRL Memorandum Report 5306**	5 MONITORING ORGANIZATION REPORT NUMBER(S)
6a NAME OF PERFORMING ORGANIZATION **Naval Research Laboratory** / 6b OFFICE SYMBOL (If applicable) **Code 4780**	7a NAME OF MONITORING ORGANIZATION
6c ADDRESS (City, State and ZIP Code) **Washington, DC 20375**	7b ADDRESS (City, State and ZIP Code)
8a NAME OF FUNDING/SPONSORING ORGANIZATION **Office of Naval Research** / 8b OFFICE SYMBOL (If applicable)	9 PROCUREMENT INSTRUMENT IDENTIFICATION NUMBER
8c ADDRESS (City, State and ZIP Code) **Arlington, VA 22217**	10 SOURCE OF FUNDING NOS. PROGRAM ELEMENT NO: **61153N** / PROJECT NO: / TASK NO: **RR033-02-44** / WORK UNIT NO: **47-0884-04**
11 TITLE (Include Security Classification) **MHD Simulation of a Comet Magnetosphere**	
12 PERSONAL AUTHOR(S) **J. A. Fedder, S. H. Brecht,* and J. G. Lyon***	
13a TYPE OF REPORT **Interim** / 13b TIME COVERED FROM **10/83** TO **10/84**	14 DATE OF REPORT (Yr., Mo., Day) **April 12, 1984** / 15 PAGE COUNT **32**
16 SUPPLEMENTARY NOTATION **This research was sponsored by the Office of Naval Research.** ***Science Applications, Inc., McLean, VA 22102**	
17 COSATI CODES FIELD / GROUP / SUB. GR	18 SUBJECT TERMS (Continue on reverse if necessary and identify by block number) **Comet tail** — **Hydrodynamics** **Cometary plasma** — **Magnetosphere**

19 ABSTRACT (Continue on reverse if necessary and identify by block number)

This paper presents results of a numerical magnetohydrodynamic (MHD) simulation of the interaction of the solar wind with a comet. We show that for a steady solar wind and interplanetary magnetic field (IMF) the cometary plasma has a distinctive structure; a spheroidal head and a long ribbon-like tail. Rotational discontinuities in the IMF lead to changes in the tail structure. We show how these effects occur and describe ray-like structures as well as a tail disconnection event. The simulation results provide a simple explanation for a number of observable features in cometary plasma tails.

20 DISTRIBUTION/AVAILABILITY OF ABSTRACT UNCLASSIFIED/UNLIMITED [X] SAME AS RPT [ ] DTIC USERS [ ]	21 ABSTRACT SECURITY CLASSIFICATION **UNCLASSIFIED**
22a NAME OF RESPONSIBLE INDIVIDUAL **J. A. Fedder**	22b TELEPHONE NUMBER (Include Area Code) **(202) 767-2875** / 22c OFFICE SYMBOL **Code 4780**

DD FORM 1473, 83 APR EDITION OF 1 JAN 73 IS OBSOLETE

SECURITY CLASSIFICATION OF THIS PAGE

CONTENTS

MHD SIMULATION OF A COMET MAGNETOSPHERE

Introduction

The approaching 1986 apparition of Comet P/Halley has generated a great deal of scientific interest and inquiry concerning the interaction of the solar wind with cometary plasmas. With the planned space probe missions to make direct measurements of Comet P/Halley plasma properties, there is considerable interest to make predictions concerning the solar wind-comet interaction. This paper presents the results of a numerical simulation of this interaction using magnetohydrodynamic (MHD) theory. Our results can be described in terms of a cometary magnetosphere owing to similarities between the comet and the earth's magnetosphere; particularly a strong magnetic field separating the cometary body and the solar wind on the bow, and a very long tenuous magnetic tail with oppositely directed field in two lobes separated by a plasma sheet and neutral field region. However, the analogy between the earth and a comet is limited as the plasma dynamical properties are considerably different.

The original concept of a cometary magnetosphere was developed by Biermann (1951), who showed that the main features of comet plasma tails could be determined by interaction with an as yet poorly understood solar wind. He also demonstrated that comets could serve a useful purpose as probes of the solar wind. The next major step in understanding the solar wind cometary interaction came from Alfvén (1957) who discussed the effect of the interplanetary magnetic field (IMF) on the interaction. Alfvén pointed out that the IMF would be "hung up" in the head of the comet and the solar wind would drag the field into a long folding tail, quite like the folding of an umbrella. Subsequent research by Marochnik (1963a,b) and Axford (1964) showed that the solar wind interaction with comets could be described by MHD theory.

Many continuing efforts considered details of the solar wind comet interation in the bow region, particularly Biermann et al. (1967), Ioffe (1966a,b; 1968a,b), Wallis (1973), Brosowski and Wegmann (1973), and Wallis and Dryer (1976). These works treated the existence of a shock in the solar wind preceeding the comet and a contact discontinuity enclosing plasma of purely cometary origin. Much of this work and a summary of results is discussed in excellent reviews by Mendis and Ip (1977), Brandt and Mendis (1979), Breus (1982), Mendis and Houpis (1982) and Ip and Axford

Manuscript approved January 31, 1984.

(1982). An excellent review of the theory of instabilities of cometary in tails has been presented in Ershkovich (1980). In a series of recent papers by Niedner and Brandt (1978, 1979), Neidner et. al. (1981), and Brandt (1982), the interaction of a dynamically changing solar wind with comet magnetospheres has been studied, particularly concerning comet ion tail dynamics and tail disconnection events.

Recently, numerical simulations of the solar wind comet interaction have been presented by Schmidt and Wegmann (1980, 1981). In these works they studied plasma flow between a hydrodynamic shock at some distance from the comet and an arbitrary fixed contact surface near the comet nucleus. Their field, flow and plasma density structure are appropriate for the inner regions of a comet magnetosphere. Unfortunately their numerical algorithm was unable to maintain divergence $\underline{B}$ identically zero over substantial regions of the simulation. Brackbill and Barnes (1980) demonstrated the serious difficulties in numerical simulations, not only in magnetic topology but also in plasma diagnostics, which can arise caused by a divergent magnetic field.

In this paper we study the solar wind interaction in the outer regions of a cometary magnetosphere. The comet acts as a source for production of plasma in the solar wind. It is seen that, as Alfvén proposed, the IMF does "hang up" in the region of the comet. The magnetic field is pulled into a long tail confining the cometary plasma. We demonstrate the configuration of field and plasma for a steady solar wind and IMF. We also explore the effect of rotational discontinuities in the IMF on the comet magnetosphere.

Mathematical and Numerical Model

We consider a solution of the ideal MHD equations on a 3 dimensional cartesian mesh (x,y,z). The equations solved numerically have the form (in gaussian units):

Continuity

$$\frac{\partial \rho}{\partial t} = -\nabla \cdot \rho \underline{v} + A \qquad (1)$$

Momentum

$$\frac{\partial \underline{v}}{\partial t} = -(\underline{v}\cdot\nabla)\underline{v} - \frac{1}{\rho}[\nabla(P+Q) + \underline{B} \times \underline{J}/c] - A/\rho\ \underline{v} \tag{2}$$

Pressure

$$\frac{\partial P}{\partial t} = -\nabla\cdot P\underline{v} - (\gamma - 1)(P + Q)\ \nabla\cdot\underline{v} + \frac{(\gamma-1)}{2} Av^2 \tag{3}$$

Ohms Law

$$\underline{E} + \underline{v} \times \underline{B}/c = 0 \tag{4}$$

Faraday's Law

$$\frac{\partial \underline{B}}{\partial t} = - c\nabla \times \underline{E} \tag{5}$$

Ampere's Law

$$\underline{J} = c\nabla \times \underline{B}/4\pi. \tag{6}$$

In these equations, ρ is the mass density, $\underline{v}$ is the plasma flow velocity, P is the plasma pressure, $\underline{E}$ is the electric intensity, $\underline{B}$ is the magnetic induction, $\underline{J}$ is the electric current density, c is the speed of light, γ is the ratio of specific heats, A is the comet plasma production rate, and Q is an artificial viscosity which is used to numerically conserve energy in the plasma (for example Q is formulated to meet jump conditions at shocks).

The method of solution is as follows: Equations (1), (2), (3), and (5) are explicitly integrated in time. Equation (4) and (6) are used to substitute for dependent variables. The numerical algorithm used is the partial donor cell method, PDM, (Hain,1978). It is a nonlinear hybrid algorithm of the shock capturing type. The PDM algorithm has been run on numerous test problems with excellent results. By careful treatment of equation (5), divergence $\underline{B}$ is identically zero throughout the simulation, thereby eliminating possible serious numerical error (Brackbill and Barnes,

1980). The numerical method has been used previously to simulate the earth's magnetosphere Brecht et al. (1981, 1982) and has shown results which agree well with theory and data.

For the comet simulation we consider an initial value problem and solve the equations in time to a quasi steady condition. The simulation is initialized on a cartesian mesh which extends from 1.4×10^6 km in front of the comet to 5×10^6 km in the antisolar direction, and to 1.25×10^6 km on each side. A steady solar wind flows in the x-direction having a velocity of 400 km/sec, a density of 5 cm^{-3}, a temperature of 5 ev and an interplanetary magnetic field of 5γ in the z direction. These values are appropriate to one astronomical unit distance from the sun. We take the cometary plasma production rate of Schmidt and Wegmann (1980) which is

$$A = \frac{m_c G\sigma}{4\pi w R^2} \exp\left(-\frac{\sigma R}{w}\right), \tag{7}$$

to gradually build up the comet. The cometary plasma production parameters in (7) are: m_c = 30 proton masses, $G = 10^{30}$ cm^{-3}, w = 1 km/sec, $\sigma = 10^{-6}$ sec^{-1}, and the radius from the comet, $R = (x^2 + y^2 + z^2)^{1/2}$. In order to study the result of asymmetric plasma production due to extinction of solar ionizing radiation we have also multiplied A by the quantity $(1 - x/R)$. This particular function was not chosen to model a specific extinction process but was used to test if extinction was important. In either case, the simulation settles down to a steady state after about 12 hours of real time.

Results

Results have been obtained for the structure of a cometary magnetosphere with both spherically symmetric and asymmetric plasma production. All results shown here are for the asymetric case since the two cases where virtually indistinguishable, both qualitatively and quantitatively. For the simulation the solar wind flows in the positive x direction. The results show a very distinct plasma tail structure for a steady solar wind and IMF. Results for a rotational discontinuity in the IMF were also obtained. These results show an indication of a tail disconnection event and also ray-like structure formation.

We begin the discussion of our results by considering the steady solar wind and IMF case. Figure 1 shows the magnetic field structure in the comet for the plane defined by the sun-comet line and the direction of the IMF. Figure 1a shows contours of magnetic field strength and 1b shows unit vectors of the field direction. The maximum magnetic field strength of 48γ occurs at a distance 1 x 10^5 km in front of nucleus. The field rises quickly to its maximum value in the head and decays very gradually into the tail where at 4 x 10^6 km behind the nucleus the strength is 11γ. The cometary plasma sheet in the tail has a magnetic field which is considerably smaller than the IMF value and is very narrow ($\sim 10^5$ km in the direction of the IMF). The field vectors demonstrate the draping of the IMF over the dense plasma in the cometary head.

Figures 2a and 2b show the flow velocity and the plasma pressure, respectively, in the plane of the IMF. The length of the velocity vectors indicates flow speed. The most striking feature of the flow pattern is that the direction of the flow is virtually unchanged from the solar wind direction throughout the cometary plasma. There is only a very slight deviation of flow which occurs at a weak shock located 2 x 10^5 km in front of the nucleus. The solar wind flow decelerates rapidly in front of and at the shock front and then reaccelerates very gradually behind the comet. In the near comet central tail the flow velocity is very low, only about 10 km/sec. In Figure 2b the perspective plot of plasma pressure shows a number of interesting features. We see the compressional heating of the solar wind flow to a few hundred eV cm^{-3} slightly ahead of and at the shock front and a cooling of the plasma behind the shock as the flow reaccelerates. There is also a very thin plasma sheet which sits in the magnetic field neutral sheet. In the plasma sheet the increased pressure is due primarily to large plasma densities and not to high plasma temperatures. The one point maximum in the pressure is artificial and denotes the nucleus of the comet.

Figures 3a and 3b show the plasma density in the comet magnetosphere. The perspective in the sun-comet - IMF (polar) plane is presented in 3a, and 3b is in the plane sun-comet perpendicular to the IMF (equatorial). In each case the single point maximum occurs at the nucleus. The striking feature in the density plots is the plasma tail.

The tail is very narrow, ~ 1 x 10^5 km, in the polar direction but quite broad in the equatorial plane. The plasma density (assuming CO_2^+) ranges from a few 100 cm^{-3} near the nucleus to a density on order 10 cm^{-3} at the mid-line of the tail 2 x 10^6 km behind the nucleus. The simulations indicate that the plasma density structure of a comet is a spheroidal head, a few times 10^5 km in diameter, with a long ribbon-like tail, 10^5 km thick in the direction of the IMF and 10^6 km wide in the equatorial plane. This characteristic plasma structure can been seen more clearly in cross-sectional contours on the plasma tail shown in Figure 4. Figures 4a, b, c, and d display plasma density contours on cross sections through the comet nucleus, as well as 2.7 x 10^5 km, 8.3 x 10^5 km, and 2 x 10^6 km behind the nucleus, respectively. The cross-section thru the nucleus shows circular contours. As the cross-sectional plane is moved tailward the contours become progressively flattened into the equatorial plane. At distances further into the tail than 10^6 km the contours describe a ribbon-like plasma structure with the small dimension in the direction of the IMF.

In the preceeding results we have shown the interesting and unique structure of a comet magnetosphere and plasma tail in a steady solar wind. The results are essentially in a steady state which was achieved after simulating 13 hours of real time. The stucture of the comet is especially sensitive to the solar wind IMF, particularly the long ribbon-like plasma tail. In the remainder of this section we will present results for the distortions caused in this structure by rotations in the IMF.

In our first study of the effect of a non steady solar wind on the cometary magnetosphere we induced a 90^o rotation of the IMF in the inflowing solar wind. The rotational discontinuity was propagated in from the front of the mesh as a one cell wide rotation of the IMF from the z direction into the y direction. The rotational discontinuity required about 1 hour to propagate to the cometary bow shock but changes in the cometary tail did not begin to show clearly until the disturbance has propagated far past the nucleus in the undisturbed solar wind. Figures 5 and 6 show the plasma densities 6 hrs and figures 7 and 8 show them 10 hrs after introduction of the rotational discontinuity. In Figure 5a, the old polar plane and new equatorial plane, we see the central remnant of the previously existing plasma tail and the formation of the new plasma sheet

in the outer regions. In 5b, the new polar plane and the old equatorial plane, we see the narrowing of the plasma tail near the nucleus and the remnant of the old plasma tail far from the nucleus. Figures 6a and 6b show more clearly how this process takes place. In 6a, which is closer to the nucleus, the plasma tail is twisting into its new orientation from the outside in, while in 6b further from the nucleus the plasma tail still has its original orientation. Figures 7 and 8, 10 hours after introduction of the rotational discontinuity, show a continuation of the process. As the rotational discontinuity propagates into the cometary magnetosphere at the plasma flow velocity, a plasma tail in the new orientation gradually is created and propagates into the comet behind the rotational discontinuity. The twist in the plasma sheet shows the location of the rotational discontinuity as it moves into the cometary magnetosphere. The flow of plasma in the comet tail remains steady and in the anti-solar direction throughout the twisting of the tail from its original position to its new orientation.

In our second study of the effect of a variable solar wind on the cometary magnetosphere we induced a 180^{o} field reversal of the IMF in the inflowing solar wind. The results for the field reversal are shown in Figures 9, 10, and 11 for times of 6, 8, and 10 hours after introduction of the field reversal, respectively. There are two distinct features which appear in the figures of the plasma density. There is a pronounced depletion of plasma density which takes place at about 10^{6} km in the anti-solar direction from nucleus. The maximum depletion is about a factor of 4 and the depletion propagates tailward with the local plasma flow velocity. The depletion appears to arise owing to small changes in the plasma flow velocity in the near comet tail which occur shortly after the field reversal reaches the shock front. The other pronounced feature is the formation of ray-like structures in the plasma tail. The ray-like structures fold with the magnetic field onto the tail plasma sheet and reenhance the plasma tail densities to the earlier values. The ray structure in the plasma density occurs at the neutral line of the IMF reversal and may be associated with a quiet form of magnetic reconnection. The plasma in the rays flows with the local convection velocity which is a ·i-sun· ·d and is virtually undisturbed from the steady values existing before ne event.

Discussion

The results presented above provide a rather simple conceptual model of a cometary magnetosphere and ion tail. The solar wind carrying an imbedded IMF encounters the comet as a massive source of ions. The cometary ions decelerate the solar wind and a weak shock is formed in front of the comet. The IMF field lines closest to the source of ionization "hang up" and are draped over the comet creating a long magnetic tail. As this process occurs the solar wind has barely deviated from the anti-solar direction and flows essentially straight on through. On each IMF field line, the region nearest the source of ionization is retarded the most and therefore continues to accumulate more ionization. After passage through the shock and cometary head the plasma reaccelerates and rarefies, but those regions passing closest to the production source and accumulating the most plasma also reaccelerate and rarify more slowly. This process leads to a cometary plasma structure with a more or less spherical head and a long tenuous ribbon-like tail: the ribbon tail being everywhere perpendicular to the local IMF. Rotations in the IMF lead to twists of the ribbon-like tail with the inner most tail regions being tied to the head by the old IMF and the outer regions of the tail oriented to the new IMF direction. IMF reversals in the simulations show a rarefaction of plasma in the tail which could be interpreted to be disconnection events and also show the formation of ray-like structures which fold onto and reenhance the tail plasma density. We will now discuss certain features and processes in more detail.

The simulation results strongly argue for weak magnetic fields in comet tails. There has been considerable disagreement on this subject in the past with Hyder et al. (1974), Ip and Mendis (1976a,b), and Mendis (1977) arguing for strong fields, and Ershkovich (1978, 1982) and the simulation by Schmidt and Wegmann (1980, 1982) arguing for smaller values. Our simulation results are definitely in agreement with the work of Ershkovich as the maximum field in the head is slightly less than a factor of 10 greater and at distances of 4×10^6 km in the tail are less than a factor of 2 greater than the IMF value. We are unaware of plasma kinetic mechanisms not included in the MHD formalism which could be responsible for enhancing the magnetic field in the cometary magnetosphere.

The results have pointed out two mechanisms which can lead to formation of ray-like structures in the comet ion tail. For the first mechanism associated with a reversal in the IMF, there is an accumulation of plasma in the comet magnetosphere along the IMF neutral line. These plasma accumulations form straight ray-like structures attached to the head of the comet. Whether this accumulation is associated with magnetic merging in the numerical model owing to numerical resistivity is at present unclear. We hope to study this question in more detail in the future. Nevertheless, the plasma enhancements do occur in the results, they fold slowly onto the tail axis and enhance the plasma density there forming a straight thin plasma tail.

The other mechanism involves the helical twisting of the thin ribbon-like plasma tail by rotational discontinuities in the IMF of less than 180^{o}. An observer viewing this twisted structure from the side would see a bright ray at positions where the ribbon-like tail was aligned with the viewing direction. These rays created by viewing perspective would also fold onto the central axis appearing to brighten the tail there also. This mechanism is similar to one described by Schmidt and Wegmann (1980, 1982), however we are unable to ascertain from their description if we have identified the same mechanism.

The thin ray-like structures and plasma tail which we identify in the simulation results all have a width of a few times 10^{5} km. This mimimum size is due solely to the resolution in the numerical grid. Structures formed in a higher resolution simulation or in a real comet could be much thinner.

Another feature of the simulation results for an IMF reversal is the suggestion of a plasma tail disconnection event as proposed and discussed by Niedner and Brandt (1978, 1979) and Niedner et al. (1981). In the simulation results we observe a decrease by about a factor of 4 in the plasma density which takes place at an anti-solar distance of about 10^{6} km from the nucleus. This plasma depletion occurs roughly 4 to 5 hours after the IMF reversal reaches the comet. It is caused by small flow velocity changes in the near comet plasma sheet which are possibly associated with pressure changes in the bow region. The plasma density decrease is not associated with magnetic reconnection in the plasma tail. Neither is it

directly associated with the IMF reversal region which is responsible for the appearance of the the ray structures off the tail axis. The depleted density region propagates in the anti-solar direction at the local plasma flow velocity, and the depleted plasma is finally replaced considerably later by folding of the rays onto the tail axis.

Since the same numerical code used for these simulations has also been used for simulations of the earth's magnetosphere (Brecht et al. 1981, 1982), it is possible to make some interesting comparisons between the two sets of results. In the case of the earth the solar wind forms a strong shock in front of the magnetosphere and deviates to flow around the magnetic obstacle, while in the case of the comet the shock is weak and the solar wind flows essentially straight on through. In the case of the earth the results show a distinct magnetopause with a clear separation of solar wind plasma and flow from that of the earth's plasma, while in the case of the comet there is no distinct separation. In the earth's magnetotail the plasma is extremely tenuous with plasma densities less than 1 cm^{-3}, while in the comet tail plasma densities are larger. The plasma sheet of the earth separating the tail lobes is a tenuous hot plasma, while in a comet the plasma sheet is a higher density cold plasma. In the case of the earth disturbances in the solar wind can lead to dynamic magnetic reconnection with high velocity plasma flows and sudden energetic acceleration events, while in the case of the comet-solar wind interaction, disturbances may lead to magnetic reconnection but the reconnection is slow and its effects are mild. It is clear that the two magnetospheres and the plasma processes in them are very different.

The reader might wonder at the remarkably different behavior of magnetic reconnection in the earth's magnetosphere and that of a comet. At least a partial answer is directly related to the orders of magnitude difference in the Alfvén speed in the two plasma tails. In the earth's magnetosphere the Alfvén speed can approach the speed of light near, and possibly even in, the magnetic neutral sheet region. In the neutral sheet region of the comet tails the Alfvén speed is orders of magnitude lower. Since the speed at which plasma flows out of the reconnection region is controlled by the Alfvén speed in the inflow region (Petschek, 1964), the plasma flow in cometary reconnection events is bound to be slow. In other

words, the magnetic field energy annihilated by reconnection must be given to the plasma. Since the β of the cometary plasma is > 1 to begin with, reconnection cannot lead to drastic changes in the plasma behavior.

In conclusion we would like to reiterate the main features of the results. The solar wind interaction with a comet leads to a magnetosphere and magnetic structure as suggested by Alfvén (1957). The magnetic field in comet tails is weak as was shown by Ershkovich (1978, 1982). The plasma density has a unique structure namely a spheroidal head stretched out in the anti-solar direction into a long ribbon-like tail Rotational discontinuities in the IMF lead to a helical twisting of the ribbon-like tail which can appear as rays in perspective. The results for the IMF reversals suggest occurrence of tail disconnections as described by Niedner and Brandt (1978, 1979) and lead to ray-like structures which fold onto the tail axis to form a new plasma tail.

ACKNOWLEDGMENTS

One of the authors, JAF, acknowledges useful discussions with W.I. Axford, A.J. Ershkovich and M.B. Niedner concerning the results of the simulations.

This research was sponsored by the Office of Naval Research.

References

Alfvén, H. (1957). On the theory of comet tails. *Tellus 9*, 92-96.

Axford, W. I. (1964). The interaction of solar wind with comets. *Planet. Space Sci. 12*, 719-720.

Biermann, L. (1951). Kometenschweife und solare Korpuskularstrahlung. *Zs. f. AP. 29*, 274-286.

Biermann, L., B. Brosowski, and H. U. Schmidt (1967). The interaction of the solar wind with a comet. *Solar Phys. 1*, 254-284.

Brackbill, J. U. and D. C. Barnes (1980). The effect of non zero $\nabla \cdot B$ on the numerical solution of the magnetohydrodynamic equations. *J. Comp. Phys. 35*, 426-430.

Brandt, J. C. (1982). Observations and dynamics of plasma tails. In *Comets* (L. Wilkering, Ed.) pp. 519-537. Univ. of Arizona Press, Tucson.

Brandt, J. C. and D. A. Mendis (1979). The interaction of the solar wind with comets. In *Solar System Plasma Physics*, Vol. II (C. F. Kennel, L. J. Lanzerotti, and E. N. Parker, Eds.) pp. 253-292. North Holland Publ. Co., Amsterdam.

Brecht, S. H., J. G. Lyon, J. A. Fedder, and K. Hain (1981). A simulation study of east-west imf effects on the magnetosphere. *Geophys. Res. Lett. 8*, 397-400.

Brecht, S. H., J. G. Lyon, J. A. Fedder, and K. Hain (1982). A time dependant three-dimensinal simulation of the earth's magnetosphere: reconnection events. *J. Geophys. Res. 87*, 6098-6108.

Breus, T. K. (1982). Solar wind interaction with comets. *Space Sci. Rev. 32*, 361-376.

Brosowski, B. and R. Wegmann (1973). Numerische behadlung eines Konetenmodells. *Meth. Verf. Moth. Phys. 8*, 125-145.

Ershkovich, A. I. (1978). The comet tail magnetic field: large or small? *Mon. Not. Roy. Astron. Soc.*, 184, 755-758.

Ershkovich, A. I. (1980). Kelvin-Helmholtz instability in Type-1 comet tails and associated phenomena. *Space Sci. Rev. 25*, 3-34.

Ershkovich, A. I. (1982). On the folding phenomenon of comet tail rays, Lab. for Astron. and Solar Phys., NASA-Goddard Space Flight Center, Greenbelt, MD, USA Mon. Not. R. Astron. Soc. (GB), Vol. 198, No.1, 297-302, Jan. 1982. *Icarus* In press.

Hain, K. (1978). The partial donor cell method. *NRL Memo Report. 3713.* Naval Res. Lab. Washington, D. C. ADA053387

Hyder, C. L., J. C. Brandt, and R. G. Roosen (1974). Tail structures far from the head of comet Kohoutek I. *Icarus 23*, 601-610.

Ioffe, Z. M. (1966). Comets in the solar wind. *Sov. Astron - AJ10*, 138-142.

Ioffe, Z. M. (1966). Comets in the solar wind, II. *Sov. Astron. - AJ10*, 517-519.

Ioffe, Z. M. (1968). Comets in the solar wind, III. *Sov. Astron - AJ11*, 668-671.

Ioffe, Z. M. (1968). Some magnetohydrodynamic effects in comets. *Sov. Astron. - AJ11*, 1044-1047.

Ip, W. H. and W. I. Axford (1982). Theories of physical process in the cometary comae and ion tails. In *Comets* (L. Wilkering, Ed.) pp. 588-634. Univ. Of Arizona Press, Tuscon.

Ip, W-H. and D. A. Mendis (1975). The cometary magnetic field and its associated electric currents. *Icarus 26*, 457-461.

Marochnik, L. S. (1963). Interaction of solar compuscular streams with cometary atmospheres, I. Shock waves in comets. *Soviet Astron. - AJ6*, 828-832.

Marochnik, L. S. (1963). Interaction between solar corpuscular streams with cometary atmospheres, II. "Collapsing" envelopes and radio-frequency emission. *Soviet Astron - AJ7*, 384-390.

Mendis, D. A. (1977). The comet-solar wind interaction. In *Study of Traveling Interplanetary Phenomena* (M. Shea, D. Smart, S. Wu, Eds) pp. 291. D. Reidal, Hingham.

Mendis, D. A. and H. L. F. Houpis (1982). The cometary atmosphere and its interaction with the solar wind. *Rev. of Geophys and Space Phys. 20*, 885-928.

Mendis, D. A. and W-H. Ip (1977). The ionospheres and plasma tails of comets. *Space Sci. Rev. 20*, 145-190.

Niedner, M. B., Jr. and J. C. Brandt (1978). Interplanetary gas, XXIII. Plasma tail disconnection events in comets: Evidence for magnetic field line reconnection at interplanetary sector boundaries. *Astrophys. J. 223*, 655-670.

Niedner, M. B. Jr. and J. C. Brandt (1979). Interplanetary gas, XXIV. Are cometary plasma tail disconnections caused by sector boundary crossings or by encounters with high-speed streams? *Astrophys. J. 234*, 723-732.

Niedner, M. B., J. A. Ionson, and J. C. Brandt (1981). Interplanetary gas, XXVI. On the reconnection of magnetic fields in cometary ionospheres at interplanetary sector boundary crossings. *Astrophys. J., 245*, 1159-1169.

Petschek, H. E. (1964). Magnetic field annihilation. *AAS-NASA Symposium on the Physics of Solar Flares. NASA Spec. Publ. SP-50*, 425.

Schmidt, H. U. and R. Wegmann (1982). Plasma flow and magnetic fields in comets. In *Comets* (L. Wilkening, Ed.) pp. 538-560. Univ. of Arizona Press, Tucson.

Schmidt, H. U. and R. Wegmann (1980). MHD - calculations for cometary plasma. *Comp. Phys. Comm. 19*, 309-326.

Wallis, M. K. (1973). Weakly-shocked flows of the solar wind plasma through atmospheres of comets and planets. *Planet. Space Sci. 21*, 1647-1660.

Wallis, M. K. and M. Dryer (1976). Sun and comets as sources in an external flow. *Astrophys. J. 205*, 895-899.

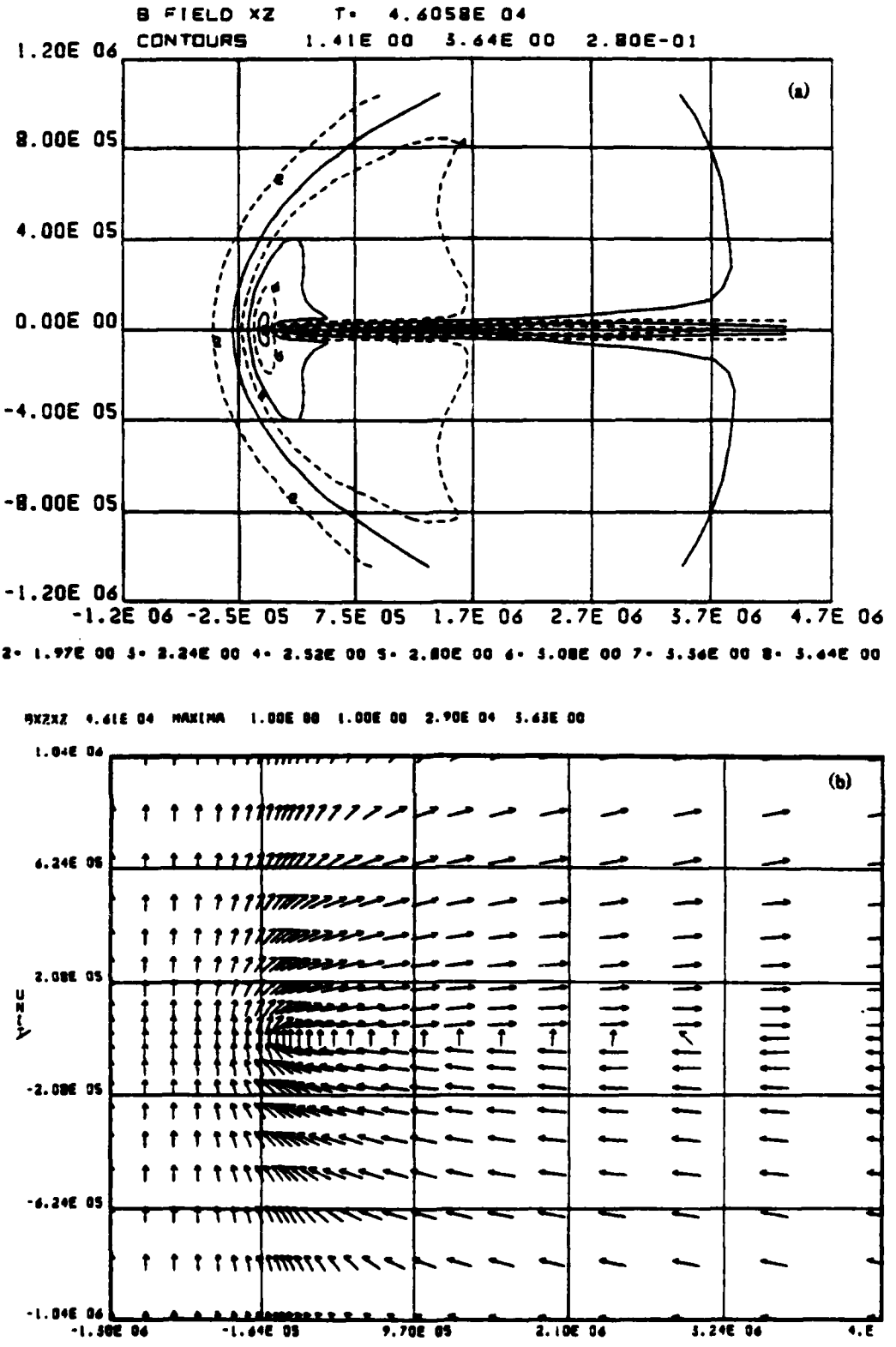

Fig. 1. Contours of magnetic field strength and vector direction in the sun-comet IMF plane. Contour levels of field strength are $2 = 7.6_{\gamma}$; $3 = 11_{\gamma}$, $4 = 16_{\gamma}$, $5 = 22_{\gamma}$, $6 = 29_{\gamma}$, $7 = 38_{\gamma}$, and $8 = 48_{\gamma}$. The comet is located at (0,0) and distances along the axis are in km.

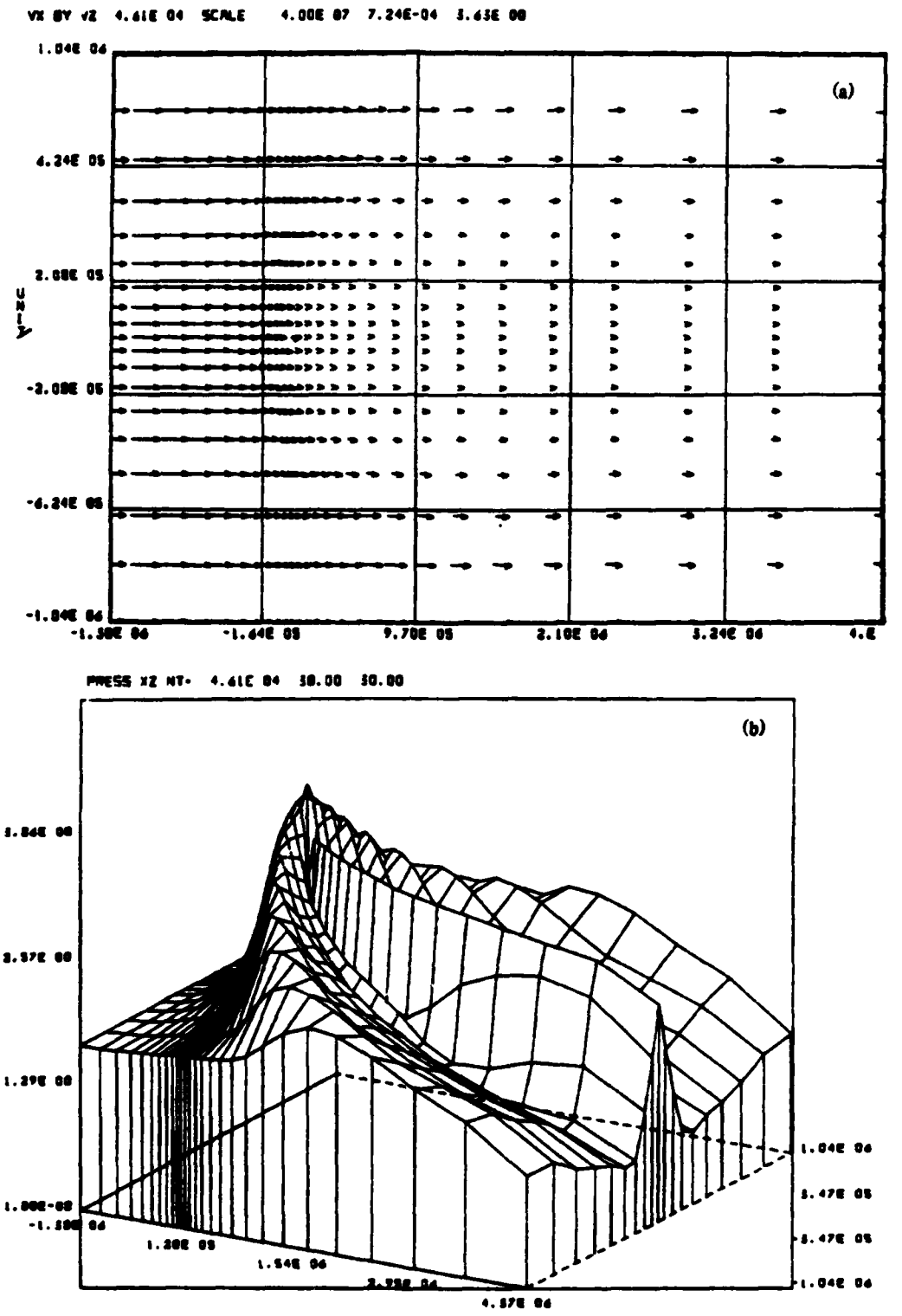

Fig. 2. Plasma flow velocity vectors, (a) and perspective plot of plasma pressure, (b). The flow velocity in the solar wind at the left edge is 400 km sec^{-1} and in the central comet is about 10 km sec^{-1}. The flow shows little deviation around comet and is essentially straight on through. The left scale on the pressure plot is the logarithm to the base 10 of pressure in eV cm^{-3}. On the pressure plot note the large pressure jump in front of and at the shock; also note the large pressures in the magnetic field null region. The single point maximum is the location of the comet nucleus and is artificial. Both plots are in the sun-comet, IMF plane.

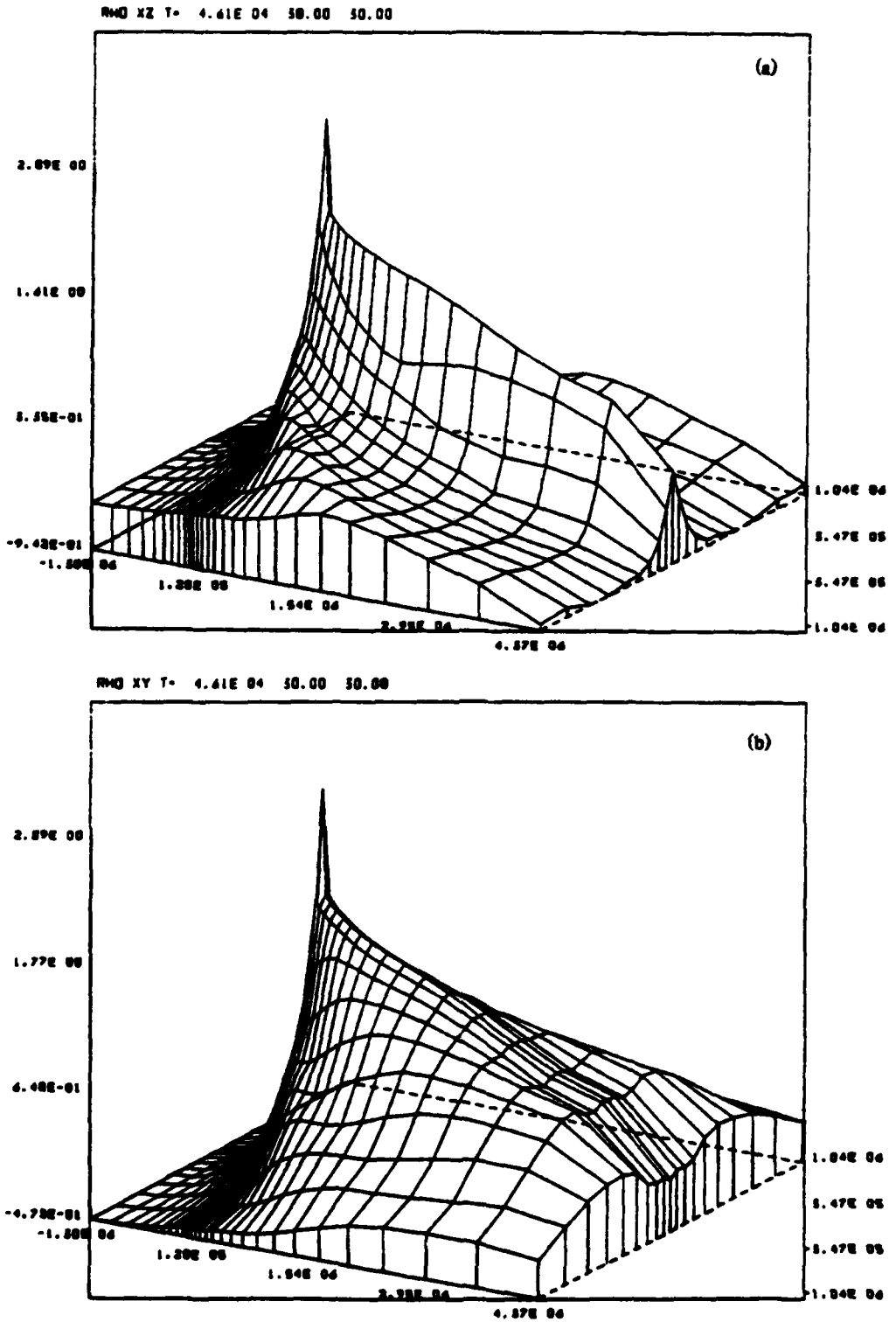

Fig. 3. Plasma density perspective plots. Diagram (a) is in the sun-comet, IMF (polar) plane, (b) is in the sun-comet perpendicular to IMF (equatorial) plane. Units on the left axis are the logarithm to the base 10 of $\rho/M(CO^+)$ in cm^{-3}. A single point maxima again locates the comet nucleus. The plasma tail is narrow in the direction of the IMF and broad perpendicular to the IMF. The plasma density 5×10^4 km from the comet nucleus is about 200 cm^{-3} and at 2×10^6 km on the anti-solar tail axis is about 10 cm^{-3}.

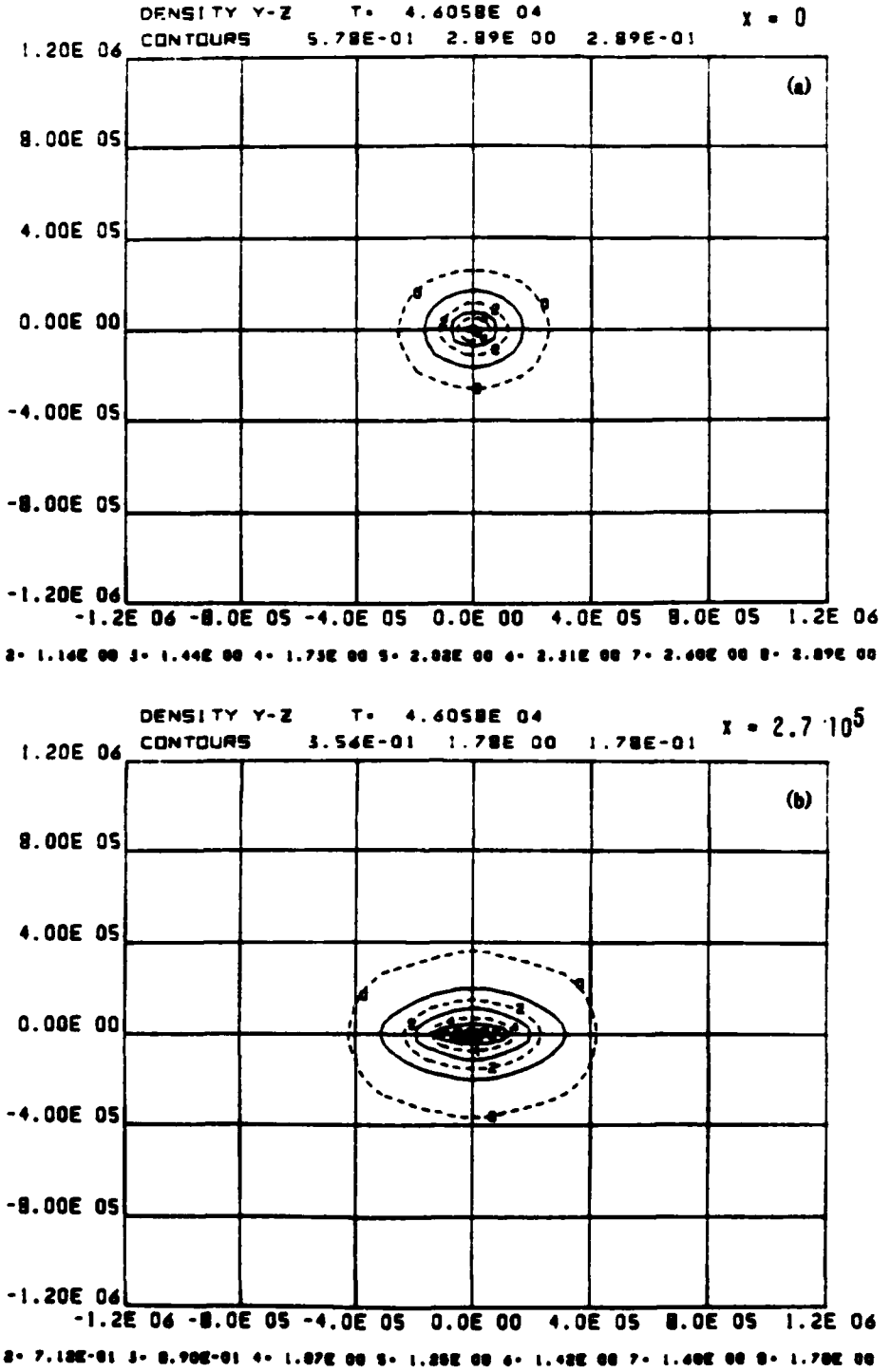

Fig. 4. Plasma density contours on cross-sectional planes through the comet and tail perpendicular to the solar wind flow. Diagram (a) shows a plane through comet nucleus, (b) is 2.7×10^5 km in the anti solar direction from the nucleus, (c) is 8.3×10^5 km in the anti solar direction, and (d) is $2. \times 10^6$ km in the anti solar direction. Notice that the plasma density contours are nearly circular in the comet head but become progressively flattened onto the equatorial plane further into the tail.

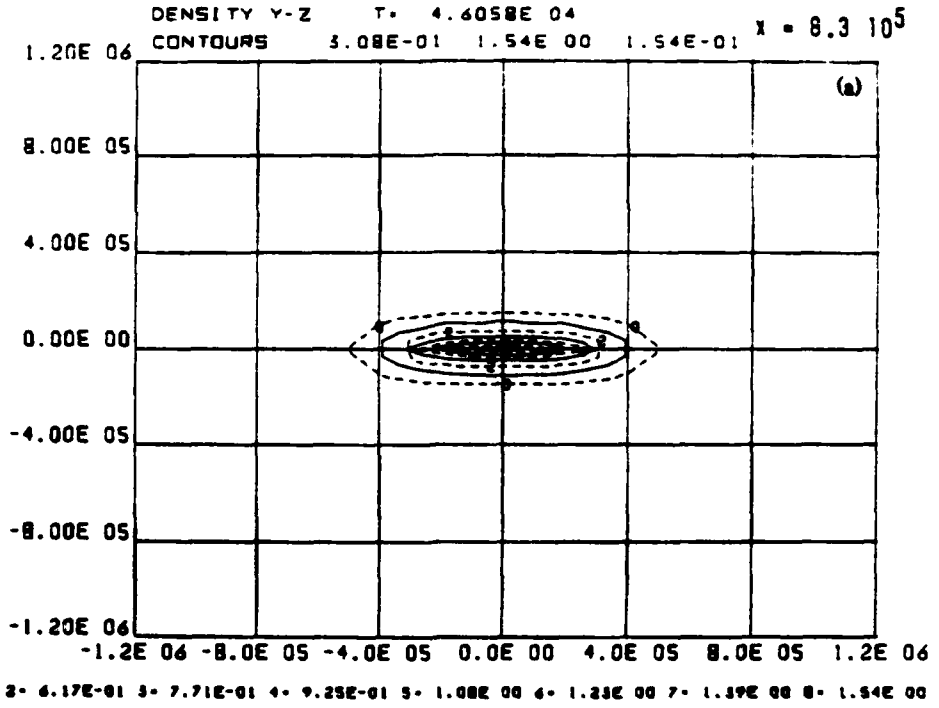

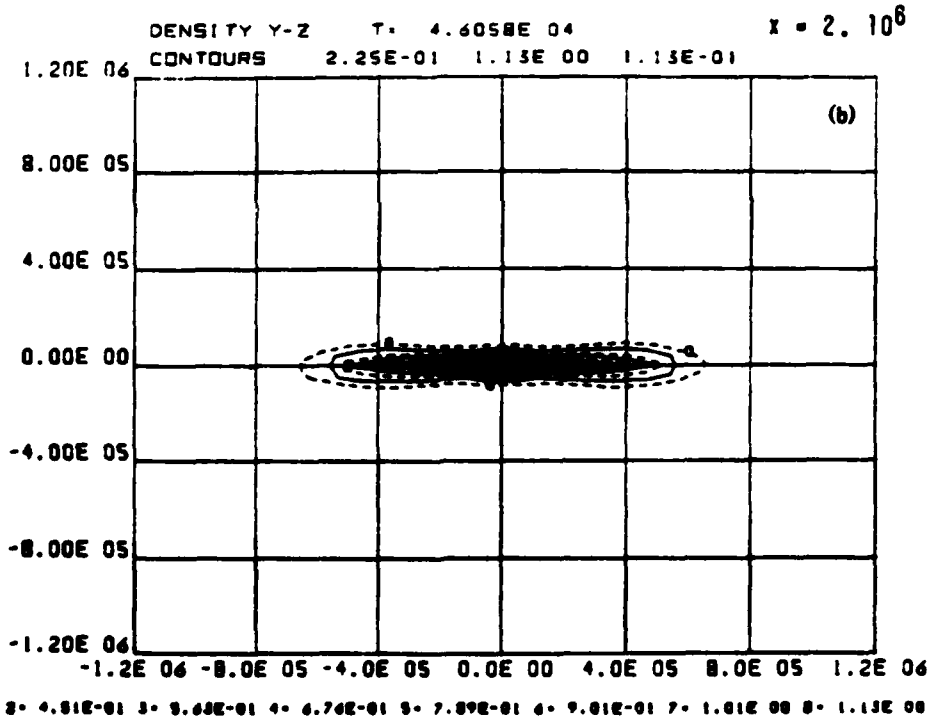

Fig. 4 (Continued. Plasma density contours on cross-sectional planes through the comet and tail perpendicular to the solar wind flow. Diagram (a) shows a plane through comet nucleus, (b) is 2.7×10^5 km in the anti solar direction from the nucleus, (c) is 8.3×10^5 km in the anti solar direction, and (d) is $2. \times 10^6$ km in the anti solar direction. Notice that the plasma density contours are nearly circular in the comet head but become progressively flattened onto the equatorial plane further into the tail.

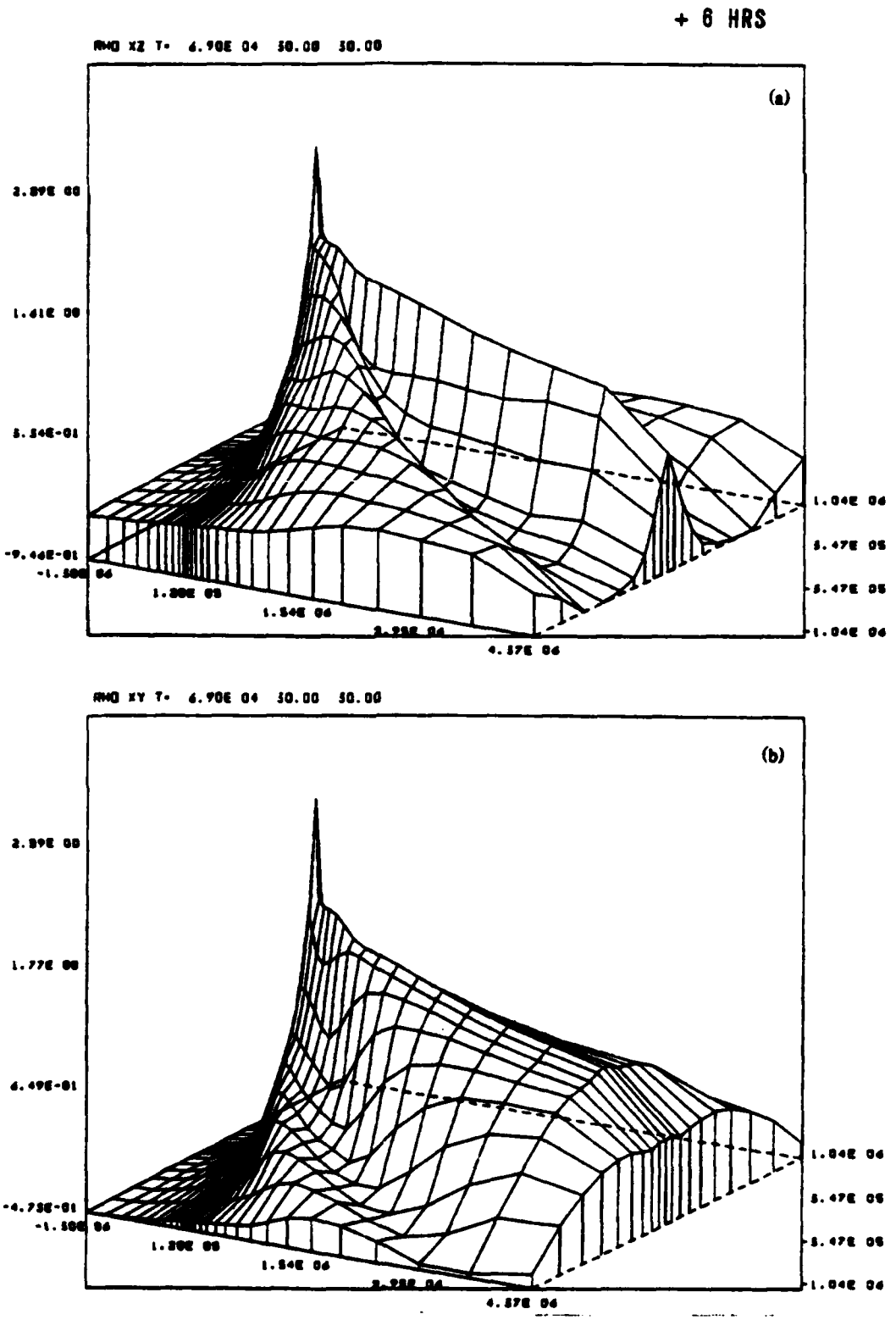

Fig. 5. Perspective plots of plasma density 6 hours after introduction of a 90° rotational discontinuity into the solar wind. Figure (a) shows the old polar, new equatorial plane, and (b) shows the new polar old equatorial plane. Note the filling of plasma from outside in (a) and the narrowing of near comet tail in (b).

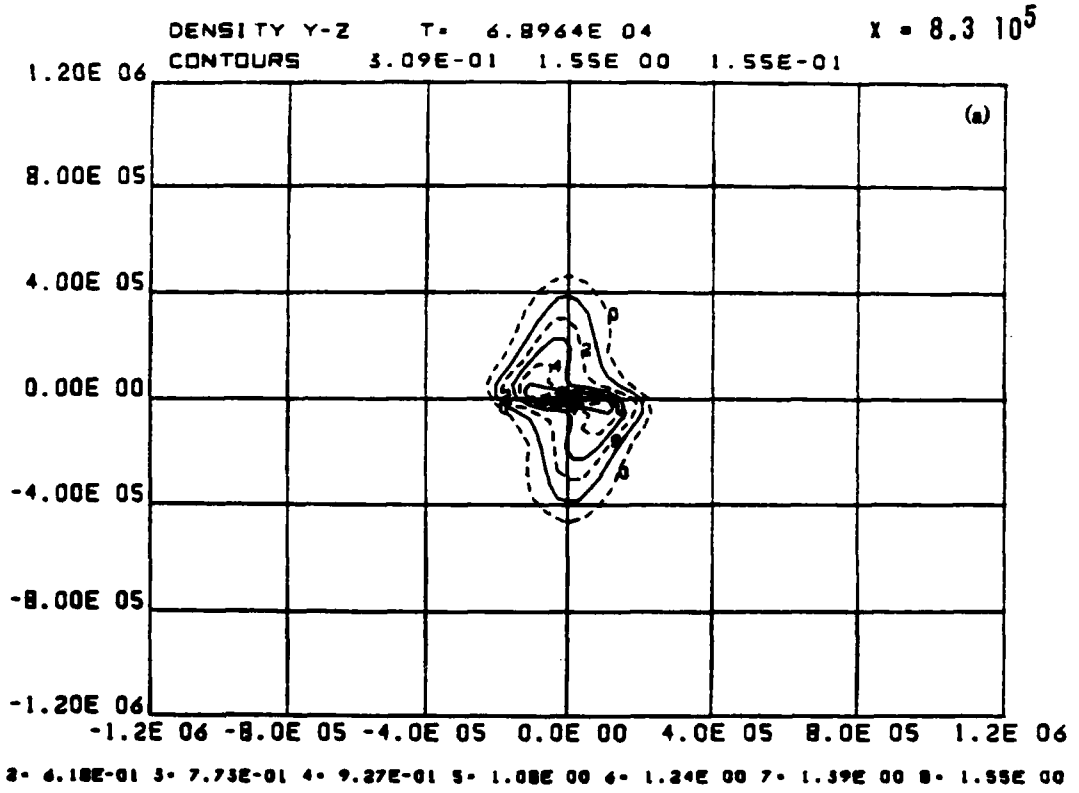

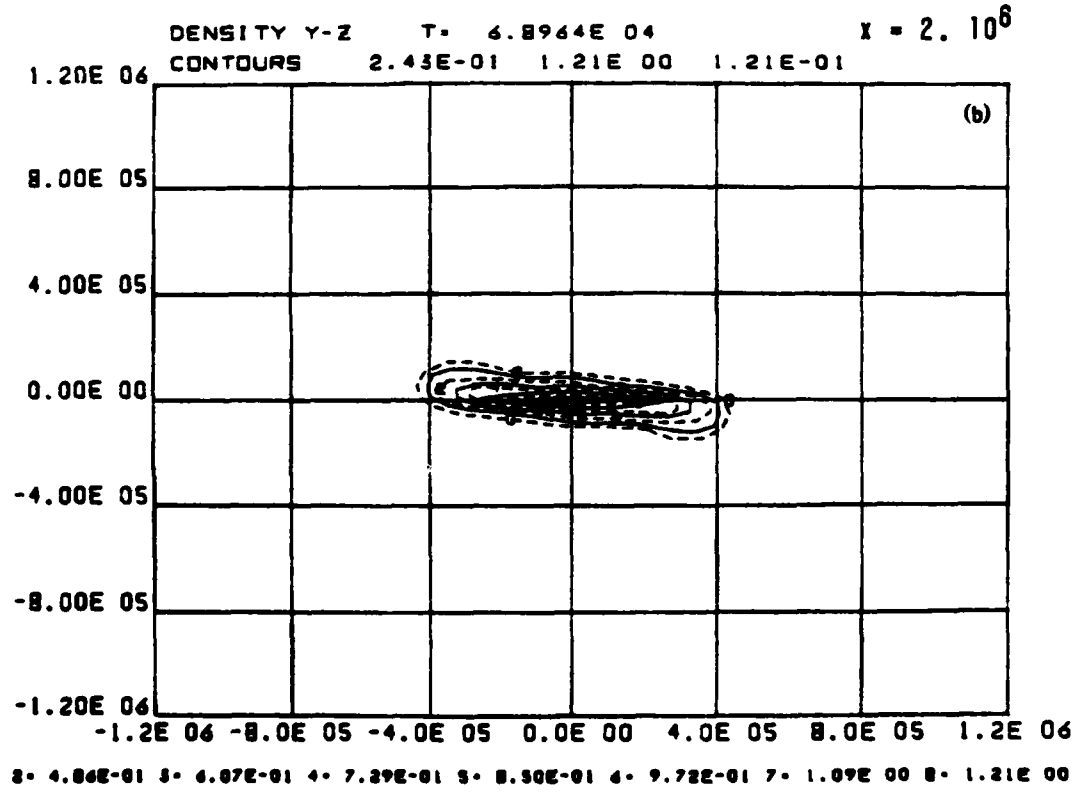

Fig. 6. Plasma density contours in cross-sectional planes perpendicular to the solar wind 6 hours after the 90° rotational discontinuity. Figure (a) shows a cross-sectional plane 8.3×10^5 km behind the comet nucleus and (b) shows a cross-sectional 2×10^6 km behind. Note the twisting of the plasma sheet from outside inward.

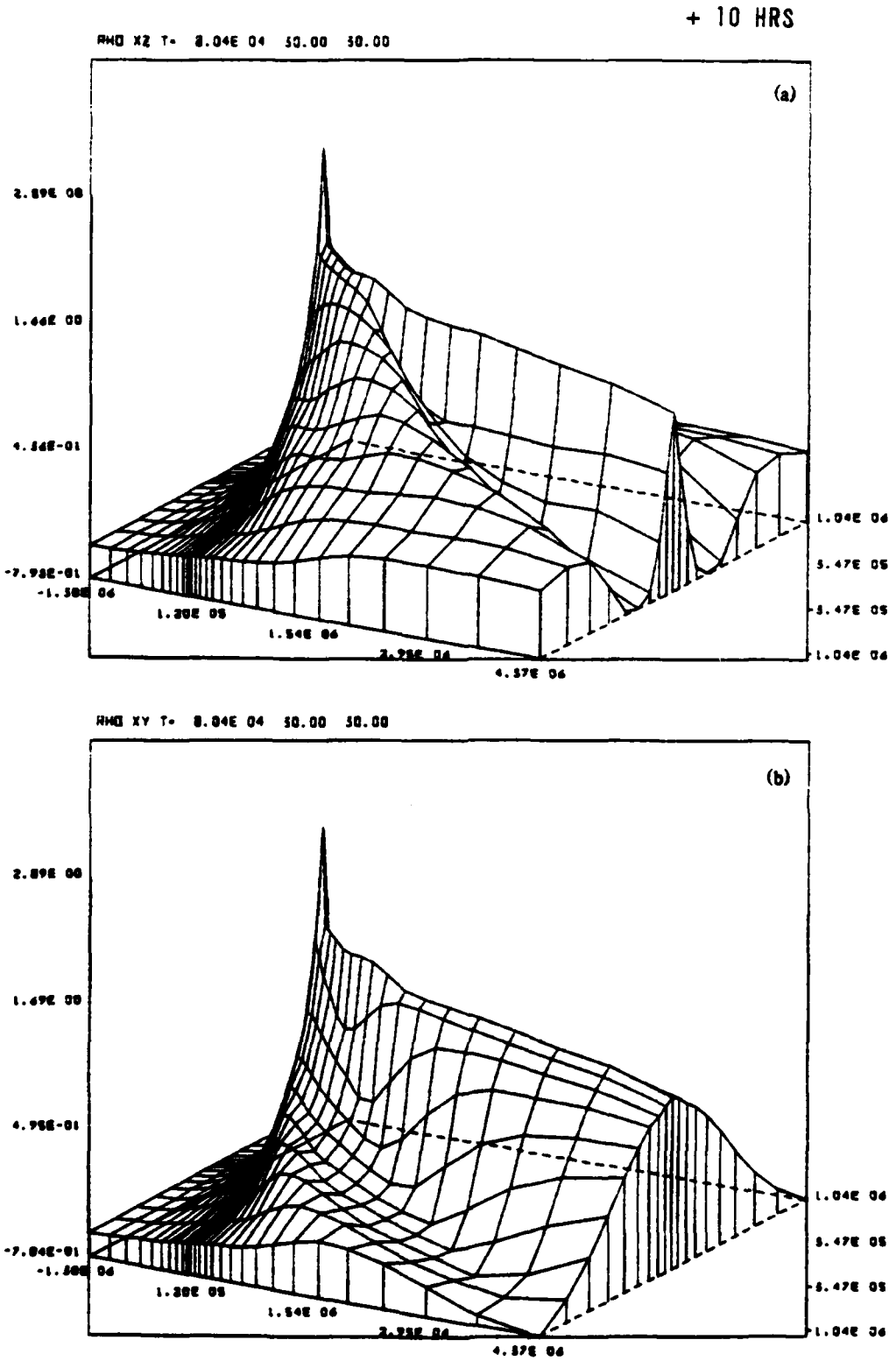

Fig. 7. Continuation of Fig. 5 plasma density for 10 hours after introduction of 90° rotational discontinuity. Notice the continual filling in plot (a) the continual thinning in plot (b).

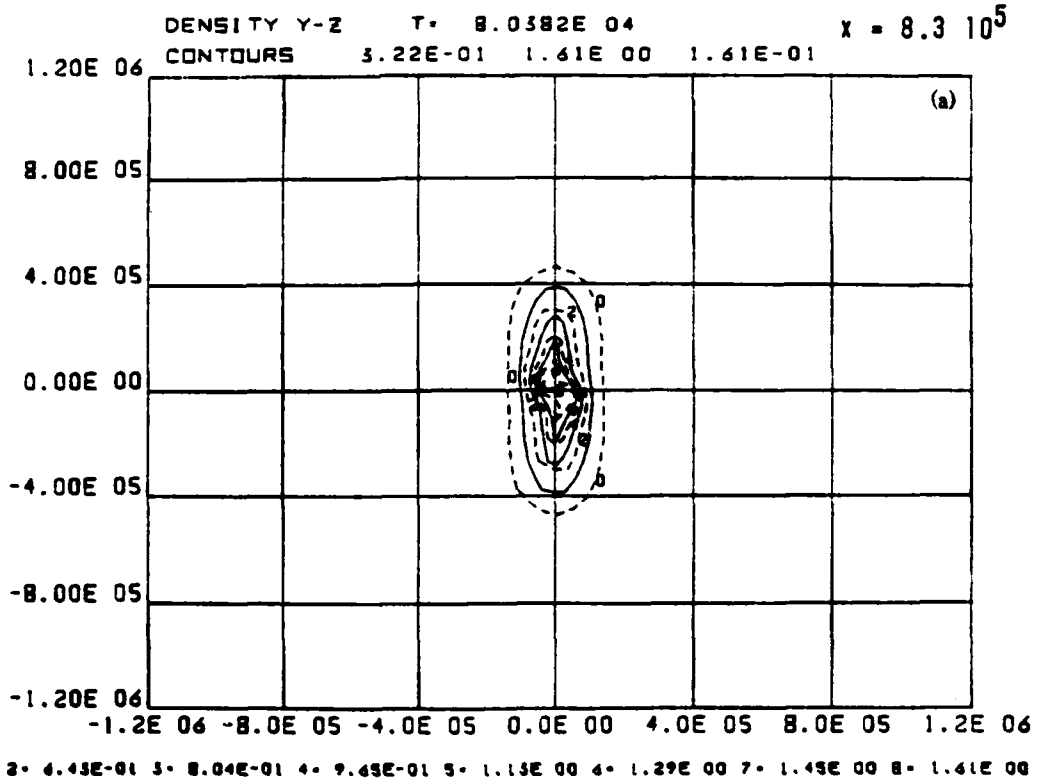

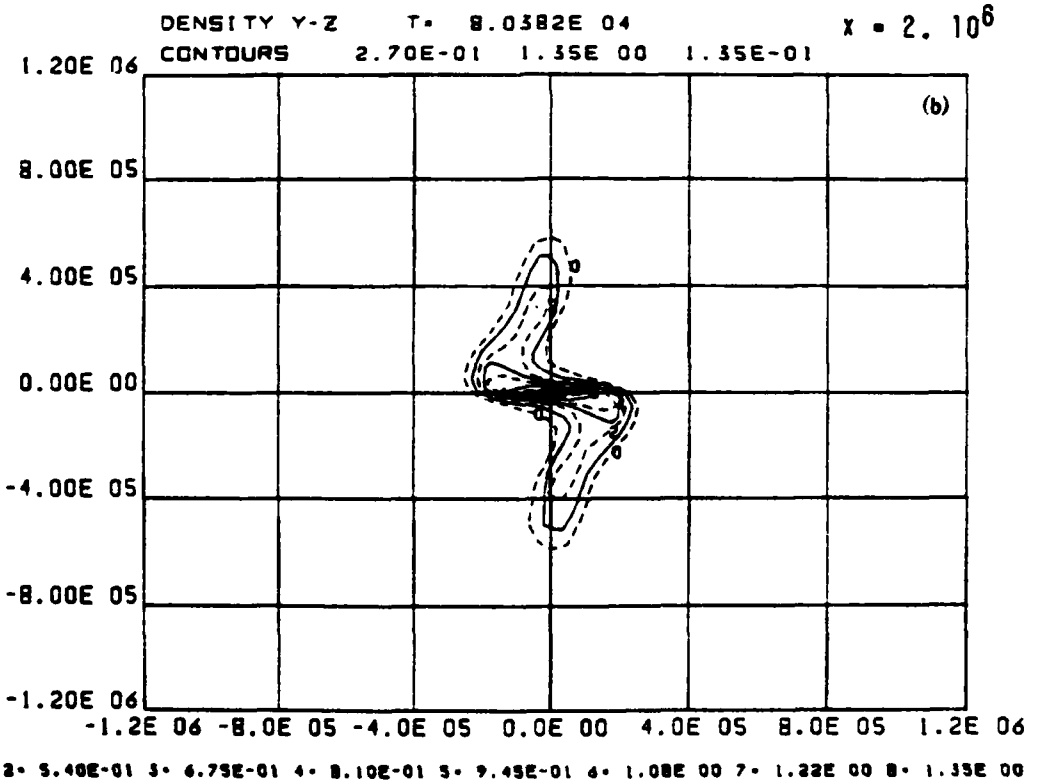

. 8. Continuation of Fig. 6 for 10 hours after rotational discontinuity. Note the gressive twisting of the comet tail plasma sheet.

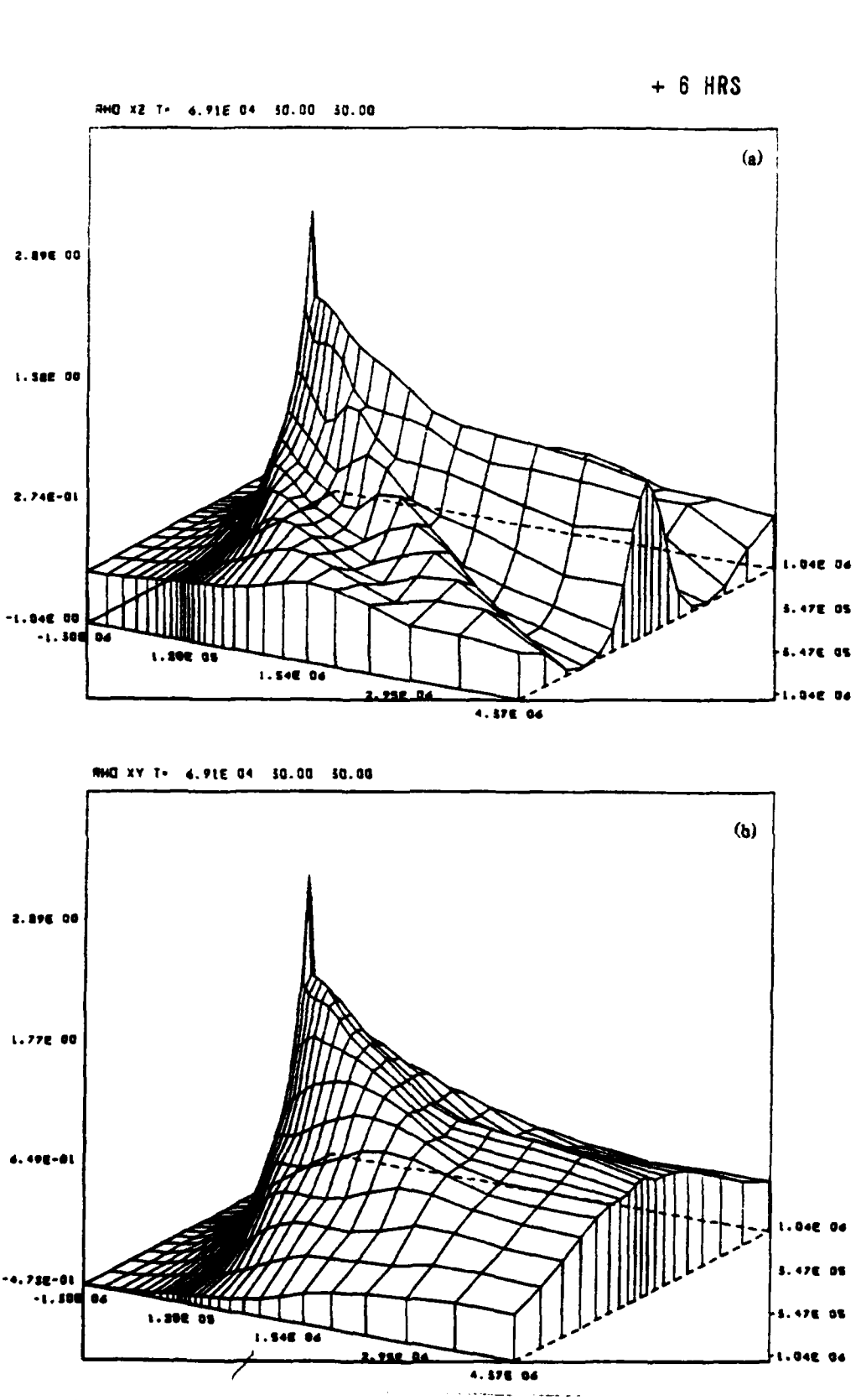

Fig. 9. Perspective plots of plasma density 6 hours after introduction of IMF reversal into the solar wind. Figure (a) shows the polar plane and (b) shows the equatorial plane. Notice the depletion in plasma density by about a factor of four at 1.5×10^6 km behind the comet. Also in diagram (a) there is the appearance of ray-like structures connected to the comet nucleus along the field reversal region in the solar wind.

= 8 HRS

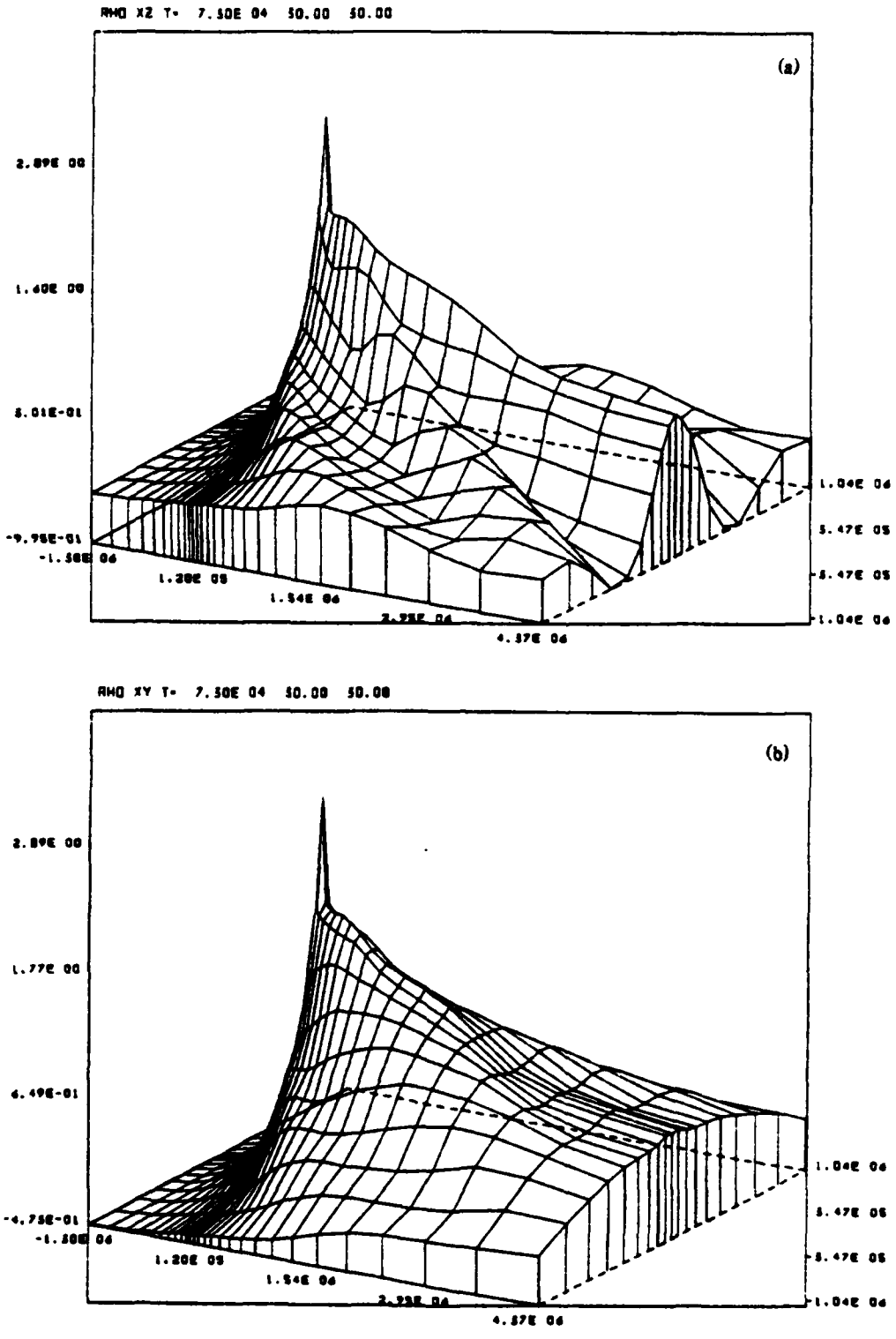

Fig. 10. A continuation of plasma density plots of Fig. 9 for 8 hours after introduction of IMF reversal. The depleted plasma region has moved tailward and the ray structures have folded closer to the axis.

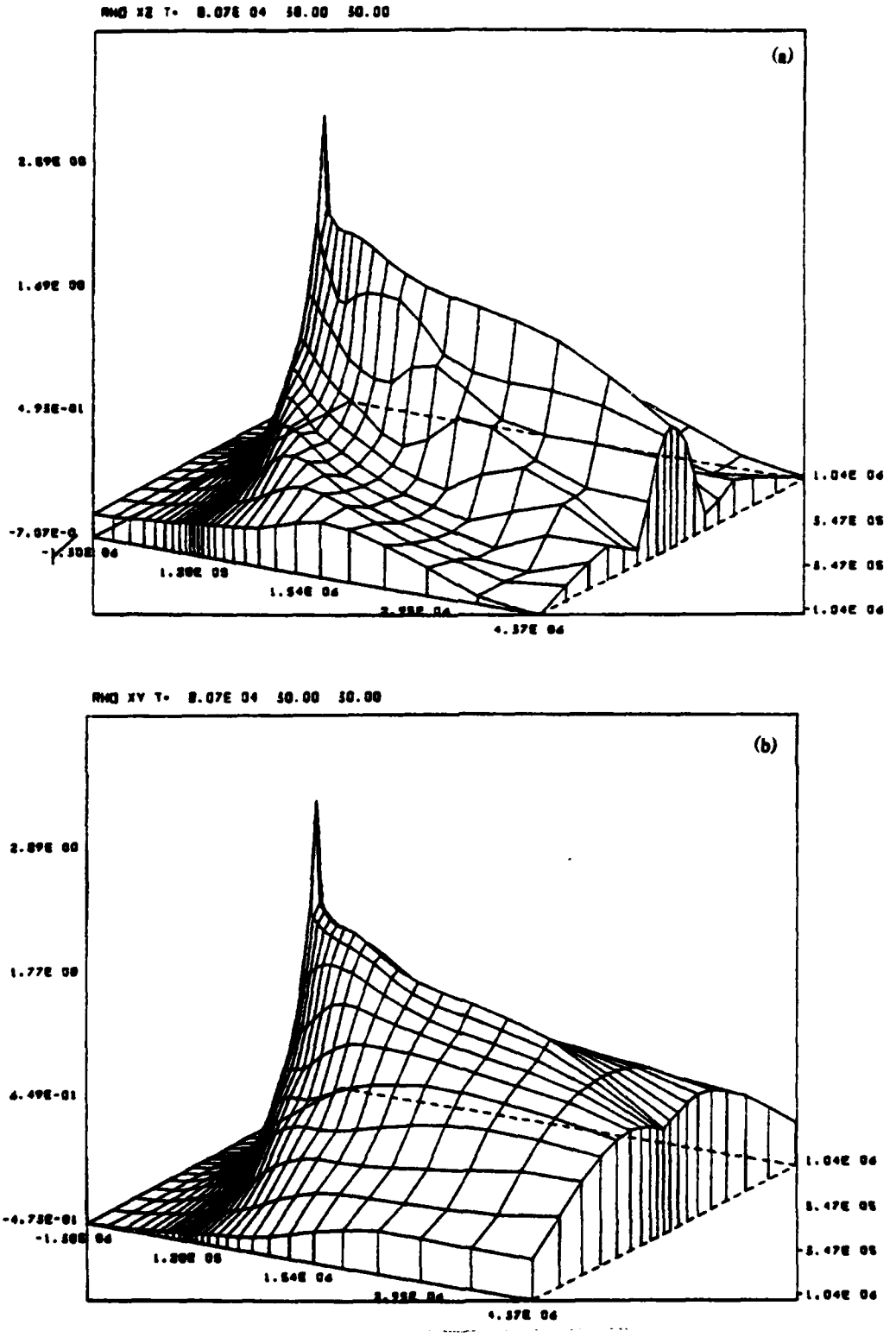

Fig. 11. A continuation of plasma density plots of Figs. 9 and 10 but for 10 hours after IMF reversal. The depleted plasma region has continued to move tailward and the ray structures continue folding.

Distribution List

Director
Naval Research Laboratory
Washington, D.C. 20375
ATTN: Code 4700 (26 Copies)
Code 4701
Code 4780 (100 copies)
Code 4187 (E. Szuszczewicz)
Code 4187 (P. Rodriguez)
Code 2628 (20 copies)
DTIC (2 copies)

University of Alaska
Geophysical Institute
Fairbanks, Alaska 99701
ATTN: Library
S. Akasofu
J. Kan
J. Roederer
L. Lee

University of Arizona
Dept. of Planetary Sciences
Tucson, Arizona 85721
ATTN: J.R. Jokipii

University of California, S.D.
LaJolla, California 92037
(Physics Dept.):
ATTN: J.A. Fejer
T. O'Neil
J. Winfrey
Library
J. Malmberg
(Dept. of Applied Sciences):
ATTN: H. Booker

University of California
Los Angeles, California 90024
(Physic Dept.):
ATTN: J.M. Dawson
B. Fried
J.G. Moralles
W. Gekelman
R. Stenzel
Y. Lee
A. Wong
F. Chen
M. Ashour-Abdalla
Library
J.M. Cornwall

(Institute of Geophysics and
Planetary Physics):
ATTN: Library
C. Kennel
F. Coroniti

Columbia University
New York, New York 10027
ATTN: R. Taussig
R.A. Gross

University of California
Berkeley, California 94720
(Space Sciences Laboratory):
ATTN: Library
M. Hudson
(Physics Dept.):
ATTN: Library
A. Kaufman
C. McKee
(Electrical Engineering Dept.):
ATTN: C.K. Birdsall

University of California
Physics Department
Irvine, California 92664
ATTN: Library
G. Benford
N. Rostoker
C. Robertson
N. Rynn

California Institute of Technology
Pasadena, California 91109
ATTN: R. Gould
L. Davis, Jr.
P. Coleman

University of Chicago
Encrico Fermi Institute
Chicago, Illinois 60637
ATTN: E.N. Parker
I. Lerche
Library

Thayer School of Engineering
Dartmouth College
Hanover, NH 03755
ATTN: Bengt U.O. Sonnerup

University of Colorado
Dept. of Astro-Geophysics
Boulder, Colorado 80302
ATTN: M. Goldman
Library

Cornell University
School of Applied and Engineering Physics
College of Engineering
Ithaca, New York 14853
ATTN: Library
R. Sudan
B. Kusse
H. Fleischmann
C. Wharton
F. Morse
R. Lovelace

Harvard University
Cambridge, Massachusetts 02138
ATTN: Harvard College Observatory
(Library)
G.S. Vaina
M. Rosenberg

Harvard University
Center for Astrophysics
60 Garden Street
Cambridge, Massachusetts 02138
ATTN: G.B. Field

University of Iowa
Iowa City, Iowa 52240
ATTN: C.K. Goertz
D. Gurnett
G. Knorr
D. Nicholson

University of Houston
Houston, Texas 77004
ATTN: Library

University of Maryland
Physics Dept.
College Park, Maryland 20742
ATTN: K. Papadopoulos
H. Rowland
C. Wu

University of Michigan
Ann Arbor, Michigan 48140
ATTN: E. Fontheim

University of Minnesota
School of Physics
Minneapolis, Minnesota 55455
ATTN: Library
J.R. Winckler
P. Kellogg

M.I.T.
Cambridge, Massachusetts 02139
ATTN: Library
(Physics Dept.):
ATTN: B. Coppi
V. George
G. Bekefi
T. Dupree
R. Davidson
(Elect. Engineering Dept.):
ATTN: R. Parker
A. Bers
L. Smullin
(R.L.E.):
ATTN: Library
(Space Science):
ATTN: Reading Room

Princeton University
Princeton, New Jersey 08540
Attn: Physics Library
Plasma Physics Lab. Library
C. Oberman
F. Perkins
T.K. Chu
H. Okuda
V. Aranasalan
H. Hendel
R. White
R. Kurlsrud
H. Furth
S. Yoshikawa
P. Rutherford

Rice University
Houston, Texas 77001
Attn: Space Science Library
R. Wolf

University of Rochester
Rochester, New York 14627
ATTN: A. Simon

Stanford University
Institute for Plasma Research
Stanford, California 94305
ATTN: Library

Stevens Institute of Technology
Hoboken, New Jersey 07030
ATTN: B. Rosen
G. Schmidt
M. Seidl

University of Texas
Austin, Texas 78712
ATTN: W. Drummond
V. Wong
D. Ross
W. Horton
D. Choi
R. Richardson
G. Leifeste

College of William and Mary
Williamsburg, Virginia 23185
Attn: F. Crownfield

Lawrence Livermore Laboratory
University of California
Livermore, California 94551
ATTN: Library
B. Kruer
J. Thomson
J. Nucholls
J. DeGroot
L. Wood
J. Emmett
B. Lasinsky
B. Langdon
R. Briggs
D. Pearlstein

Los Alamos National Laboratory
P.O. Box 1663
Los Alamos, New Mexico 87545
ATTN: Library
D. Forslund
J. Kindel
B. Bezzerides
H. Dreicer
J. Ingraham
R. Boyer
C. Nielson
E. Lindman
L. Thode

N.O.A.A.
325 Broadway S.
Boulder, Colorado 80302
ATTN: J. Weinstock
Thomas Moore (SEL, R-43)
W. Bernstein
D. Williams

Sandia Laboratories
Albuquerque, New Mexico 87115
ATTN: A. Toepfer
G. Yeonas
D. VanDevender
J. Freeman
T. Wright

Bell Laboratories
Murray Hill, New Jersey 07974
ATTN: A. Hasegawa

Lockheed Research Laboratory
Palo Alto, California 94304
ATTN: M. Walt
J. Cladis
J. Siambis

Physics International Co.
2400 Merced Street
San Leandro, California 94577
ATTN: J. Benford
S. Putnam
S. Stalings
T. Young

Science Applications, Inc.
Lab. of Applied Plasma Studeis
P.O. Box 2351
LaJolla, California 92037
ATTN: L. Linson
J. McBride

Goddard Space Flight Center
Greenbelt, Maryland 20771
ATTN: M. Goldstein
T. Northrop
T. Birmingham

TRW Space and Technology Group
Space Science Dept.
Building R-1, Room 1170
One Space Park
Redondo Beach, California 90278
ATTN: R. Fredericks
W.L. Taylor

National Science Foundation
Atmospheric Research Section (ST)
Washington, D.C. 20550
ATTN: D. Peacock

Goddard Space Flight Center
Code 961
Greenbelt, Maryland 20771
ATTN: Robert F. Benson

NASA Headquarters
Code EE-8
Washington, D.C. 20546
ATTN: Dr. E. Schmerling
Dr. J. Lynch
Dr. D. Butler

Klumpar, David
Center for Space Sciences
P.O. Box 688
University of Texas
Richardson, Texas 75080

Leung, Philip
Dept. of Physics
University of California
405 Hilgard Avenue
Los Angeles, California 90024

Lysak, Robert
School of Physics and Astronomy
University of Minnesota
Minneapolis, MN 55455

Schulz, Michael
Aerospace Corp.
A6/2451, P.O. Box 92957
Los Angeles, California 90009

Shawhan, Stanley
Dept. of Physics & Astronomy
University of Iowa
Iowa City, Iowa 52242

Temerin, Michael
Space Science Lab.
University of California
Berkeley, California 94720

Vlahos, Loukas
Dept. of Physics
University of Maryland
College Park, Maryland 20742

Matthews, David
IPST
University of Maryland
College Park, Maryland 20742

Schunk, Robert W.
Utah State University
Dept. of Physics
Logan, Utah 84322

Director,
Department of Energy
ER20:GTN, High Energy &
Nuclear Physics
Washington, D.C. 20545
ATTN: Dr. Terry Godlove

Director,
Department of Energy
Office of Inertial Fusion
Washington, D.C. 20545
ATTN: Dr. Richard Schriever

Director
Defense Nuclear Agency
Washington, D.C. 20305
ATTN: Dr. Leon Wittwer
Dr. P. Crowley
Dr. Carl Fitz